Int. J. Multiphase Flow Vol. 15, No. 1, pp. 1–21, 1989
Printed in Great Britain.

0301-9322/89 $3.00 + 0.00

STATISTICAL CHARACTERISTICS OF FREE FALLING FILMS AT HIGH REYNOLDS NUMBERS

T. D. KARAPANTSIOS,† S. V. PARAS and A. J. KARABELAS‡
Department of Chemical Engineering, University of Thessaloniki, 540 06 Thessaloniki, Greece

(*Received* 6 *August* 1987; *in revised form* 11 *September* 1988)

Abstract—The characteristics of films flowing inside a vertical pipe are studied experimentally. Using an accurate wire conductance technique the film thickness is measured over the Re range 509–13,090. The mean film thickness data are in good overall agreement with established relations. Extensive statistical analysis shows that film thickness fluctuations have a stochastic character. The description given by Dukler and co-workers, of a relatively well-defined substrate in between the large waves, is confirmed up to $\mathrm{Re} \approx 7000$. At higher Re the substrate tends to lose its identity, due to amplification of the small waves on its surface. Moreover, data on standard deviation, h_{max} and h_{min} indicate that at $\mathrm{Re} > 5000$ the amplification of large waves essentially stops, and that the substrate thickness tends to increase. The calculated probability density functions of film thickness, the spectral density functions, the skewness and kurtosis provide new reliable information for the statistical description of film thickness fluctuations. Finally, by identifying the wave peaks it is found that the total number of waves is nearly constant, in the range of Re studied, and that the distribution of wave peaks becomes bimodal at $\mathrm{Re} \gtrsim 4000$.

Key Words: film thickness, waves, substrate, experimental data, fluctuations, statistical analysis, probability density, spectra

1. INTRODUCTION

The interface characteristics of thin falling films are of interest to designers of process equipment and, among others, to researchers attempting to model annular two-phase flow. Even the simple case considered here, namely free falling films with no interfacial shear, is of considerable practical significance as, for example, in modeling heat transfer operations (e.g. Mudawwar & El-Masri 1986). It is not, therefore, surprising that a large body of literature exists on this topic, dating back to the early part of this century (Nusselt 1916). Despite this wealth of information it is generally recognized (e.g. Dukler 1977; Maron *et al.* 1985) that there are serious gaps in our knowledge which hamper our ability to predict the characteristics of wavy free falling films.

Perhaps the most important publications on this topic so far are those of Dukler and his students (Telles & Dukler 1970; Chu & Dukler 1974, 1975), who stressed the random character of film thickness variation with time and presented meaningful statistical analyses of it. Chu & Dukler (1974, 1975), using more refined techniques than those of Telles & Dukler (1970), interpreted their data in terms of two main classes of random waves; i.e. *large* waves which carry a significant portion of all flowing liquid and *small* waves which cover the substrate that exists between large waves. A method relying on the measured mean film thickness, $\bar{h}$, was employed to make this classification and to extract the statistics of each wave class from the measured probability density distribution of the time series $h(t)$.

The thorough statistical analysis of small and large waves, performed by Chu & Dukler, provided new insight into the mechanisms of falling film flow and suggested ways of theoretically attacking this problem. The fairly successful effort by Maron *et al.* (1985) to model the interface structure of free falling films is a direct outcome of the above work.

Despite the above very positive contributions made by Chu & Dukler (1974, 1975), their film thickness measurements seem to be in error, giving much smaller mean values (especially at high Re) compared to other data and to well-established relations. This has already been pointed out by Henstock & Hanratty (1976) and evidence is given in this paper and in Maron *et al.* (1985), e.g. data appearing in their figure 6. One could attribute this problem to the limited sensitivity of

†Present address: Department of Chemical Engineering, University of Rochester, Rochester, NY 14627, U.S.A.
‡To whom all correspondence should be addressed.

their conductivity probes which were mounted flush with the pipe wall and could respond well only to very thin films.

In another interesting experimental study by Takahama & Kato (1980), emphasis was given to the longitudinal flow characteristics of falling films. Water flowed on the outer wall of a vertical pipe and the thickness variation with time was measured by "needle contact" and "electrical capacity" probes. Aside from the work of Chu & Dukler, this was the only other published study, available to us, in which significant statistical analysis of vertical falling films was presented. The influence of distance x, from the liquid entry point, on the film flow characteristics was found to be very important over a pipe length $x = 1.70$ m. However, most of the statistical parameters computed by Takahama & Kato indicated that the distance x at which the wavy film reached a fully developed structure was not far from their last measuring station, $x = 1.7$ m.

The main objective of the work reported here was to obtain accurate measurements of film thickness variation with time, over a wide range of Re, using the "parallel-wire conductance" probe—a different technique from that employed by Chu & Dukler (1974, 1975) and Takahama & Kato (1980). These new measurements would be used to complement the data from the above studies, to make the necessary comparisons with them and, by statistical analysis, to provide results improving our fundamental understanding of thin film flow.

The experiments were performed with water in a 50 mm i.d. Plexiglas pipe. Measurements were made at a location $x = 2.50$ m from the entry. This location was considered sufficient to obtain a nearly well-developed wave structure, for small viscosity fluids and for Re values not far from those of Takahama & Kato (1980).

When the experimental part of this work was almost complete, a thesis by Zabaras (1985) became available to us. The "parallel-wire conductance" probe was used for film thickness measurements. In addition to tap water a potassium ferri- and ferro-cyanide solution was employed as the flowing medium, allowing simultaneous wall shear stress measurements with the well-known electrochemical technique (Son & Hanratty 1969).

The measurements made by Zabaras provided useful information on the response of the local wall stress to the wave motion. A strong length effect was also noticed, as in the study of Takahama & Kato (1980). However, no attempt was made to resolve the question of pipe length necessary to reach a fully developed wave structure. Comparisons of our data with some data by Zabaras are presented here.

In the main part of this paper, visual observations are outlined first and some remarks on flow patterns are made on the basis of the film thickness traces. Attention is given next to the mean film thickness data. Finally, the results of the statistical analysis are presented and discussed.

Throughout this paper the Reynolds number is defined as $\mathrm{Re} = 4\Gamma/\nu$, where Γ is the circumferential film flow rate per unit width (L^2/T) and ν is the kinematic viscosity.

2. EXPERIMENTAL EQUIPMENT AND TECHNIQUES

2.1. Flow system

The main vertical pipe consisted of four Plexiglas sections of total length 2.80 m: the inlet section (0.30 m), the flow development section (2.0 m), the test section (0.25 m), on which the probes were mounted, and the outlet section (0.25 m). Special care was taken to obtain almost perfect alignment and fitting of the flanged sections, by machining tongues and grooves into each pair of flanges. The pipe i.d. in the test section was 50 mm $\pm$ 0.01.

The pipe was supported on a rigid laboratory metal frame at two points, to insure perfect vertical alignment. Measurements with a precision instrument used in land surveying (theodolite), before and after the tests, showed a mean deviation of $<0.01^\circ$ from the vertical.

Tap water was used either directly for high flow rates, or recirculated with a centrifugal pump for flow rates below 21 l/min. Two Fisher–Porter flowmeters covered the range of our experiments ($\sim$11 to $\sim$321 l/min). Flow adjustment was achieved with a combination of valves and a by-pass. A cooler was used to control the temperature in the case of water recirculation. The tap water was filtered to remove particles $>5\,\mu$m.

Water from the flowmeters was led to the feeding vessel by means of a flexible hose to eliminate possible vibrations caused by the pump and the flow system. A special cylindrical feeding vessel was used with the inlet section of the vertical pipe, located at the centerline of the vessel, forming a weir. To insure uniform film formation and to minimize disturbances at the entrance, the inlet section (weir) was tapered over a length of ~ 10 cm. Care was also taken to minimize liquid agitation in the feeding vessel by using a multiple liquid entry into it. Water from the vertical pipe fell into an open receiving vessel, with provisions to avoid air bubble formation. The flow system was very similar to that employed by Dukler and co-workers; e.g. Zabaras (1985).

2.2. Experimental technique

The "parallel-wire conductance probe" technique was used in this investigation. It was originally employed by Swanson (1966) and later extensively used by Hanratty and his students (e.g. Miya *et al.* 1971; Andritsos 1986), who refined the signal electronic analyzer in order to improve the accuracy and sensitivity of the technique for very small thickness measurements.

A Plexiglas test section was fabricated, with special removable plugs made of the same material. Two kinds of probes were made using the plugs, i.e. "parallel-wire" probes and flush mounted "hot-film" probes for wall shear stress measurements. Technical difficulties prevented the use of the latter probes in this investigation. Eight (8) plug positions were machined around the test-section circumference, spaced at 45° intervals. The plugs were located at two pipe cross sections, 45 mm apart, making available a total of 16 probe positions for possible use.

Three "parallel-wire" probes were fabricated. The intention was to use them simultaneously, However, in preliminary tests an interaction of the electric fields of two neighboring probes was noticed, resulting in a reduction of the signal. Therefore, only one probe was used at a time to obtain the following data sets at two locations:

Data set A. Probe position at $\varphi = 0°$ and distance from water inlet $x = 2.52$ m.
Data set B. Probe at $\varphi = 180°$ and distance from inlet $x = 2.475$ m.

Here the angle φ indicates only the relative probe position for the two sets.

Each probe consists of a pair of short parallel wires glued in a plug. The chromel wires have a dia ~ 0.5 mm, a length of ~ 2 cm and are spaced 2 mm apart. These short and *rigid* wires, fixed in a removable plug, are considered much better suited for our type of experiments than much thinner wires which require a different type of support. Their main advantage is that they allow the probes (plugs) to be removed and calibrated easily outside the test section. Obviously, one may consider as a disadvantage the relatively large wire diameter which may introduce some error in their response. However, additional tests carried out with the 0.5 mm probes and with another type of specially designed probes, of dia 0.1 mm, showed that the probes employed in this work had an excellent response.

It should be pointed out here that with the thinner wires the signal is weaker, requiring greater amplification and introducing errors due to electronic noise. Moreover, the calibration of thin probes is usually made in the test section, which is tedious and error prone.

The parallel-wire conductance technique is based on the inverse proportionality between electrical resistance and liquid layer thickness covering the wires. An electronic signal analyzer is needed to make film thickness measurements. An a.c. carrier voltage of 25 kHz frequency is applied across the probes and the analyzer converts the response, due to film thickness variation, to an analog output signal.

The signal analyzer circuit employed in this study was designed at the University of Illinois (e.g. Andritsos 1986). Only relatively minor modifications were made in the units constructed in our laboratory (Paras 1988). Each probe could be connected to a separate analyzer unit to permit simultaneous film measurements. Testing and calibration of each analyzer was made before each set of measurements by using precision resistors. The output voltage was found to vary linearly with resistance across the wires, almost in the entire range of resistances used (1.2–525 kΩ).

Probe calibration was carried out outside the test section. The plug with the parallel wires was fixed on a precision micrometer. By precisely measuring (within ± 0.01 mm) the changes in the depth of immersion of the wires in water and the corresponding changes of output voltage, a linear relationship was obtained. Calibration measurements for depths of immersion < 0.5 mm were not

made to avoid errors due to meniscus formation at the wire/stagnant water interface. Thus, the linear calibration relationship was extrapolated to zero film thickness in order to cover the range 0–0.5 mm. This procedure proved to be very satisfactory and the calibration lines very reproducible. The sensitivity of the measuring technique, including the digitization error is estimated to be 0.002 mm. This sensitivity was achieved by trying various settings of the electronic analyzer in conjunction with various procedures of probe calibration. The accuracy of the technique was estimated to be 0.020 mm.

2.3. Data collection

The conductivity of tap water was measured before and after each run. It was around 450 μS throughout the tests. The temperature was $20.0 \pm 0.1^{\circ}$C.

The analog output signal from the analyzer was fed to an A/D converter (Interactive Structures, type AI13) connected to an Apple IIe microcomputer (128 kbyte RAM, 6502 processor), having a real time clock (Interactive Structures, type DI09). A Macintosh plus microcomputer (1 Mbyte RAM, processor 68000 with 20 Mbyte hard disk and an 800 kbyte floppy disk) was used for final data analysis and presentation.

Data were taken over a time period of 8 s. A sampling frequency of 500 Hz was selected after some trial runs showing that only with sampling frequencies <150 Hz at high Re the recorded signal was not representative of the true film thickness variation. The mean film thickness value was used as a criterion to judge the adequecy of sampling frequency and sample size. The sampling frequency was almost an order of magnitude higher than the greatest frequencies observed in the time series $h(t)$. The details of data storage and treatment are given in a thesis by one of the authors (Karapantsios 1987). The data obtained in this study are stored in diskettes for possible future use.

3. OBSERVATIONS OF INTERFACIAL WAVES

Visual observations were made and pictures were taken using light pulses of short duration from a stroboscope. At the smallest Re achieved in this study (Re = 509), waves were observed with a relatively large front in the lateral direction. These appeared to be followed by a train of progressively smaller waves. The shape of the large wave front in the lateral direction appeared to be roughly sinusoidal. Similar wave fronts were photographed by Pierson & Whitaker (1977) at smaller Re. Occasional merging of the above waves was observed. However, overall there seemed to be considerable order in the wave structure. Another noteworthy feature at Re = 509 is the large number of "calm" regions (patches) on the film with no waves or ripples. The film flow at this Re is usually considered to be laminar.

At higher flow rates ($\mathrm{Re} \approx 1100$) the "calm" regions are reduced in area and frequency of appearance. Similarly, the size of previously outlined wave fronts is reduced, and the merging of waves becomes more frequent. Nevertheless, there is still some order in the wave structure.

At still higher Re (≈ 1700), the calm regions appear very seldom, the fairly regularly spaced large waves are fewer and the merging of waves leads to film disturbances of a random nature. It seems that at this Re the film flow is at, or past, the transition to another flow regime of a more random character.

At Re = 2900 the random character of film flow is pronounced. One also observes large waves moving with a velocity greater than the rest of the film. The film flow at this Re is usually considered to be turbulent. For Re = 3000 to 5000 the same pattern prevails with a somewhat higher frequency of appearance of large waves.

At Re = 6700 the large waves appear to have a well-pronounced two-dimensional form; i.e. their front covers a substantial portion of the pipe circumference. This pattern is in agreement with a description presented by Chu & Dukler (1975). Similar waves were observed at $\mathrm{Re} \approx 9000$.

In addition to the above visual observations it is useful, for the following statistical analysis, to review the salient features of film flow displayed in the traces from the conductance probes. Figure 1 shows traces at the lowest and highest Re obtained in our experiments, i.e. Re = 509 and

13,090, respectively. The mean film thickness in each case is marked with a straight line in this figure.

Relatively large amplitude waves, or "roll" waves are evident in all the traces. Moreover, one can recognize:

- The *substrate*, a region of small thickness in between the large waves. Small amplitude waves cover the substrate.
- The front of the large waves usually starts from the substrate and has a steep slope.
- The back of these waves has a smaller slope and may extend down to the substrate.

The above remarks are in general agreement with the remarks first made by Dukler and his students (Telles & Dukler 1970; Chu & Dukler 1974; Zabaras 1985). It must be pointed out, however, that at high Re (especially above ~ 8000) the random character of film thickness fluctuation appears to be strong, the "small" waves on the substrate are greatly amplified, and it is difficult to distinguish them from the so-called "large" waves. Figure 1 for Re = 13,090 is one such example.

At first sight, the traces in figure 1 give the false impression that there is a large increase of film surface area due to the waves. However, using the mean velocity $\bar{U} = Q/\pi D\bar{h}$, to change the time scale to a length scale, it becomes evident that even the largest waves have a length very much greater than their amplitude. Consequently, calculations for various Re, using the above mean velocity $\bar{U}$, show a film surface area greater by only 0.1–0.2% relative to the surface corresponding to the mean thickness. Blass (1979) and Takahama & Kato (1980) have calculated a surface increase due to the waves of $<3\%$ and $<0.03\%$, respectively.

4. MEAN FILM THICKNESS

In figure 2 the data from this investigation are compared with those from seven other studies (i.e. Jackson 1955; Brauer 1956; Belkin *et al.* 1959; Portalski 1963; Dukler & Bergelin 1952; Takahama & Kato 1980; Zabaras 1985). The mean film thickness appears to be the same for vertical flat plates and for flow outside or inside a vertical pipe, as is also discussed by Blass (1979), provided the ratio of film thickness to pipe diameter is very small.

Our data are in good agreement with those of Takahama & Kato (1980), Belkin *et al.* (1959) and Portalski (1963). The data by Brauer (1956), Jackson (1955) and Zabaras (1985) are quite low, in particular above Re = 1500 where the flow is considered to be turbulent and the Nusselt (1916) relationship applying to laminar flow underpredicts $\bar{h}$. Curiously enough, Zabaras (1985) uses the Nusselt relationship to compare with his data up to Re = 4500, and his measurements are considerably lower than ours although the same experimental technique was employed in both studies—but with a different test fluid in most runs.

Figure 3 shows that the two data sets obtained in this study (see section 2.2) are in good overall agreement with predictions based on the model by Koziol *et al.* (1981). This model is a modification of the method proposed by Dukler & Bergelin (1952). However, the two models give practically identical results, except at low Re(<800) where the Koziol *et al.* model tends to approach asymptotically the Nusselt line. The data are also in good agreement with relations proposed by Henstock & Hanratty (1976) and Takahama & Kato (1980), among others.

Our data for Re < 1000 are *higher* than the Nusselt predictions. This trend is also shown in the work of Portalski & Clegg (1972) and Takahama & Kato (1980). However, other data at low Re (e.g. Dukler & Bergelin 1952) show mean thickness values below the Nusselt predictions. Additionally, in a theoretical study Kapitsa (1964) concludes that regular waves tend to reduce the mean thickness below that for a calm surface. The new data presented here cannot resolve this difference for low Re.

The systematic deviation of data set B from set A (figure 3) is difficult to explain, despite several tests with two different probes which confirmed the reproducibility of these data. We suspect that a minor inaccuracy in the pipe above the test section (position B)—possibly a slightly oval pipe cross section—may have caused this discrepancy.

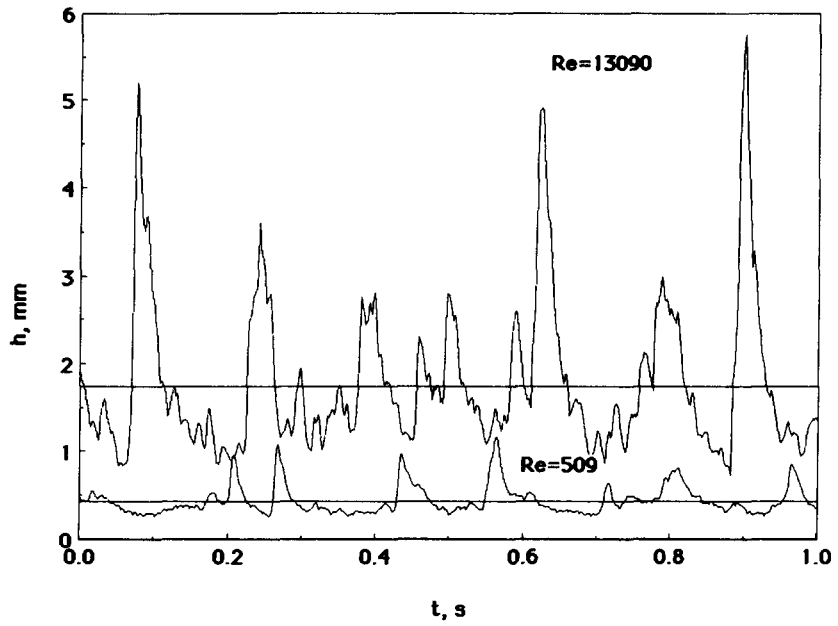

Figure 1. Film thickness traces and their mean values at Re = 509 and 13,090.

5. STATISTICAL ANALYSIS

5.1. Statistical quantities

The instantaneous film thickness $h(t)$ is considered to be a random fluctuating quantity, as shown in the recorded traces. It is further assumed that this stochastic process of film fluctuation is stationary and ergodic. Using time series analysis the following statistical parameters are obtained from the data. Mean film thickness $\bar{h}$, central moments m_i, probability density function $P(h)$, cumulative probability density function $F(h)$, autocorrelation function $R_h(r)$, autocovariance $C_h(r)$, spectral density function $G_h(f)$, as well as some combinations of the above parameters such

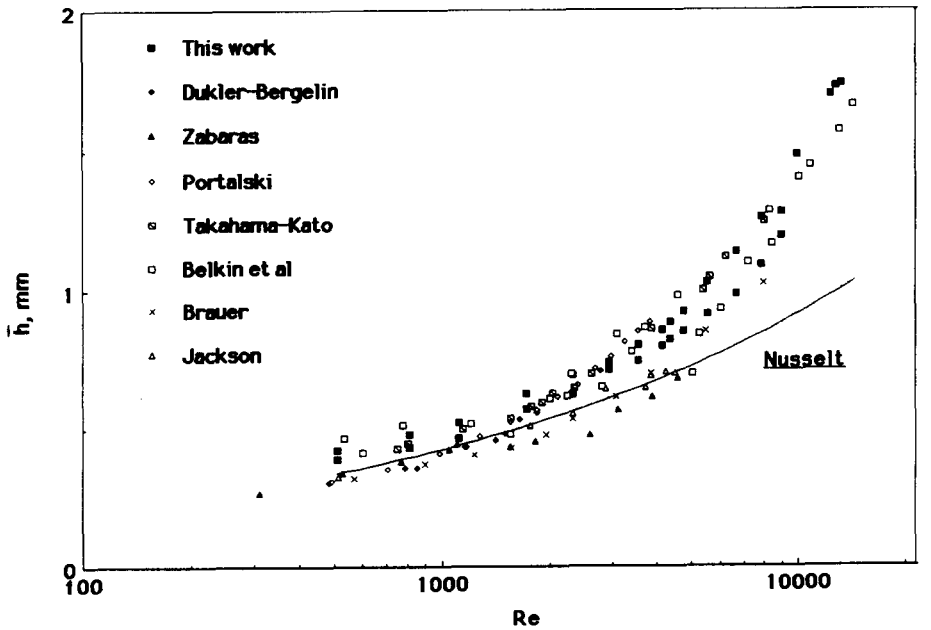

Figure 2. Comparison of data from this study with data from other investigations for small liquid viscosities.

as moment coefficients of skewness (a_3) and of kurtosis (a_4). These quantities are defined as follows (e.g. Bendot & Piersol 1971):

$$P(h) = \lim_{\Delta h \to 0} \frac{\text{Prob}\{h < h(t) < h + \Delta h\}}{\Delta h} = \lim_{\Delta h \to 0} \left(\lim_{T \to \infty} \frac{T_h}{T} \right), \quad [1]$$

$$\tilde{F}(h) = \text{Prob}\{h(t) \leqslant h\}, \quad [2]$$

$$f(h) = \frac{\mathrm{d}\tilde{F}(h)}{\mathrm{d}h}, \quad [3]$$

$$\bar{h} = \int_{-\infty}^{\infty} h \cdot f(h) \cdot \mathrm{d}h \quad [4]$$

and

$$m_i = \int_{-\infty}^{\infty} (h - \bar{h})^i \cdot f(h) \cdot \mathrm{d}h, \qquad i \geqslant 2. \quad [5]$$

For the case of a data sample in continuous or discrete form the above expressions are modified accordingly; e.g. the mean value is obtained from

$$\bar{h} = \lim_{T \to \infty} \frac{1}{T} \int_0^T h(t) \cdot \mathrm{d}t \quad \text{or} \quad \bar{h} = \frac{1}{N} \sum_{i=1}^{\infty} h_i(t). \quad [6]$$

Similarly, the other parameters are

$$R_h(h) = \lim_{T \to \infty} \frac{1}{T} \int_0^T h(t) \cdot h(t + r) \cdot \mathrm{d}t, \quad [7]$$

$$C_h(r) = \lim_{T \to \infty} \frac{1}{T} \int_0^T [h(t) - \bar{h}] \cdot [h(t + r) - \bar{h}] \cdot \mathrm{d}t \quad [8]$$

and

$$G_h(f) = \int_{-\infty}^{\infty} R_h(r) \cdot \mathrm{e}^{-j \cdot 2\pi f r} \, \mathrm{d}r. \quad [9]$$

To calculate the above parameters from the measurements a 4000-point sample was used. It was obtained over a period of 8 s with a sampling frequency of 500 Hz.

5.2. Standard deviation

The root-mean-square (r.m.s.) of the fluctuations or standard deviation s, of a data sample is the positive square root of the second central moment, as defined above, and provides a measure of the "dispersion" of data about their mean value. Figure 4 shows the influence of Re on standard deviation, which is significant up to $\text{Re} \simeq 5000$. At higher Re there is a leveling-off, i.e. a small increase of s over the range $\text{Re} = 5000$ to 13090.

Relatively large r.m.s. values, such as those obtained in our study, are also reported by Takahama & Kato (1980) for $x \approx 1.7$ m, as shown in their figure 12. However, the r.m.s. values presented by Zabaras (1985) in his figure 3.8 are small, e.g. $s \approx 0.25$ mm at $x = 1.94$ m and $\text{Re} = 4500$.

Figure 5 shows the effect of Reynolds number on the ratio $s/\bar{h}$, otherwise referred to as "coefficient of variation". Several remarks can be made on the basis of these data:

- Throughout the Re range the standard deviation s is of the same order of magnitude as the mean thickness $\bar{h}$.
- A maximum value of the coefficient $s/\bar{h}$ is observed between $\text{Re} \approx 4000$ and $\text{Re} \approx 5000$. Furthermore, it is interesting that a substantial *reduction* of the ratio

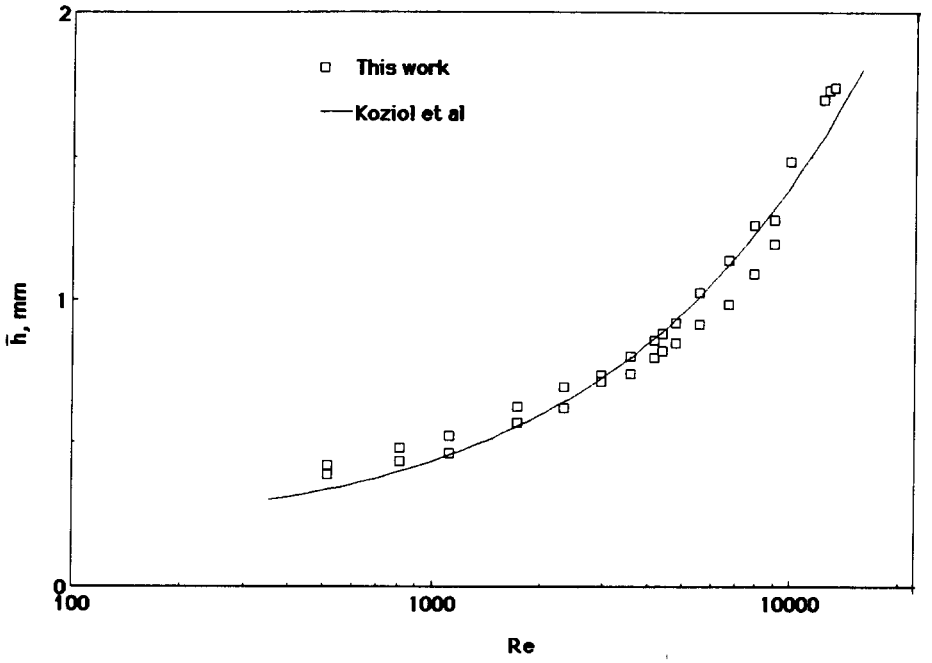

Figure 3. Comparison of mean film thickness data from this study with predictions from Koziol *et al.* (1981).

$s/\bar{h}$ takes place for Re $\gtrsim$ 5000. It may be suggested that at this Re a possible upper limit is reached for the growth or amplification of waves.

- It will be pointed out here that Telles & Dukler (1970) report data of $s/\bar{h}$ which appear to be nearly constant (around 0.73), or even slightly increasing with Re, over the range Re $\approx$ 2500 to $\sim$6000.

5.3. Maximum and minimum film thickness

Figure 6 presents the maximum h_{max}, minimum h_{min} and mean $\bar{h}$ film thickness variation with Re. The h_{max} and h_{min} data are the extreme values found in each sample. The reproducibility of the h_{max} and h_{min} data may be questioned due to the random character of the film fluctuations. However, the rigorously defined quantities $h(99\%)$ and $h(1\%)$, or $h(95\%)$ and $h(5\%)$ corresponding to thicknesses with probability of occurrence 99, 1, 95 and 5%, respectively—not presented here due to space limitations—display the same general trends as those in figure 6.

There is one order of magnitude difference between h_{max} and h_{min}. The maximum values tend to increase continuously, displaying a strong dependence on Re. However, above Re $\approx$ 5000 there is a noticeable reduction in this dependence. The minimum values remain essentially constant (at $h_{min} \approx 0.25$ mm) up to Re = 5000, exhibiting a small (nearly linear) increase at higher Re. This is better shown in figure 7. The data by Takahama & Kato (their figure 7) taken at $x = 1.7$ m, for Re = 170 to 4000, show the same value, $h_{min} \approx 0.25$ mm, as in our work.

Another interesting observation is that the ratio of mean to maximum thickness, $\bar{h}/h_{max}$ or $\bar{h}/h(99\%)$, remains practically unchanged over the Re range of our measurements, as shown in figure 8. This may be attributed to the strong effect of the large waves on the mean value $\bar{h}$. The h_{max} and $h(99\%)$ values correspond to peak values of large waves, thus providing a rough measure of large wave amplitude.

5.4. Probability density distributions

Figure 9 shows four measured distributions covering the Re range of our experiments. As already observed by previous investigators, all the distributions obtained are asymmetric with a long tail to the right, i.e. *skewed to the right*. Therefore, they are expected to have a *positive* skewness. An

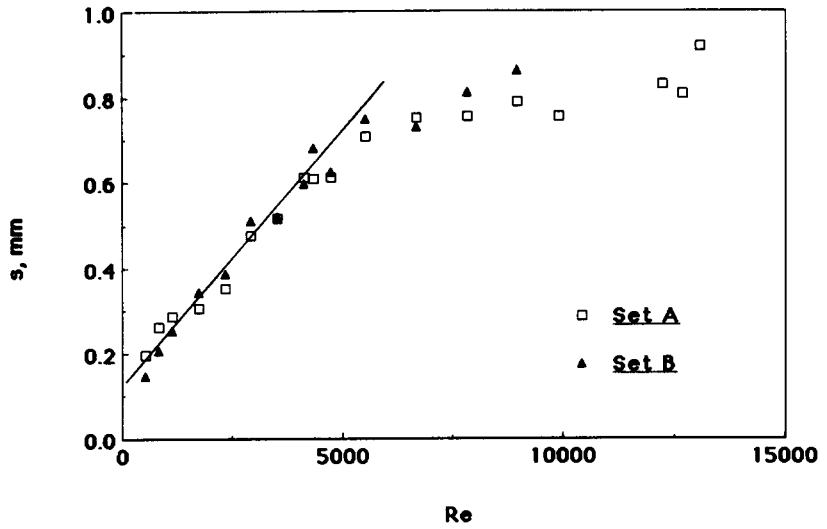

Figure 4. The influence of Re on the standard deviation, s, of film thickness fluctuations.

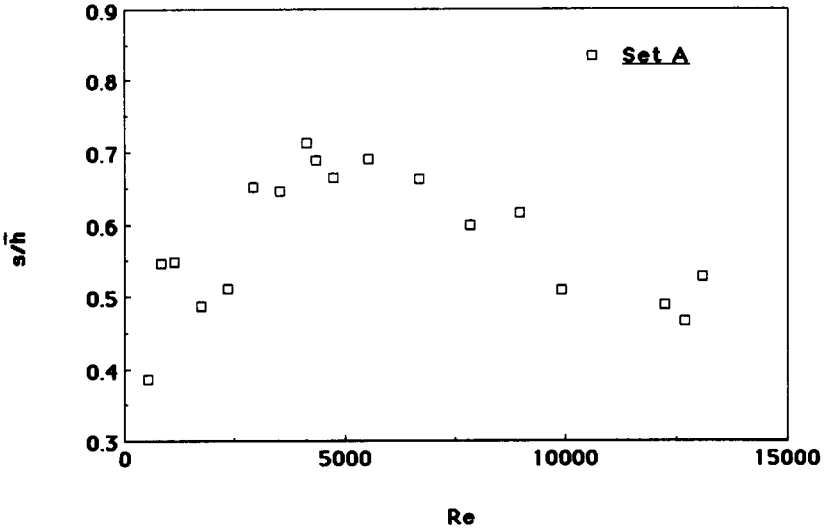

Figure 5. The effect of Re on the coefficient of variation $s/\bar{h}$.

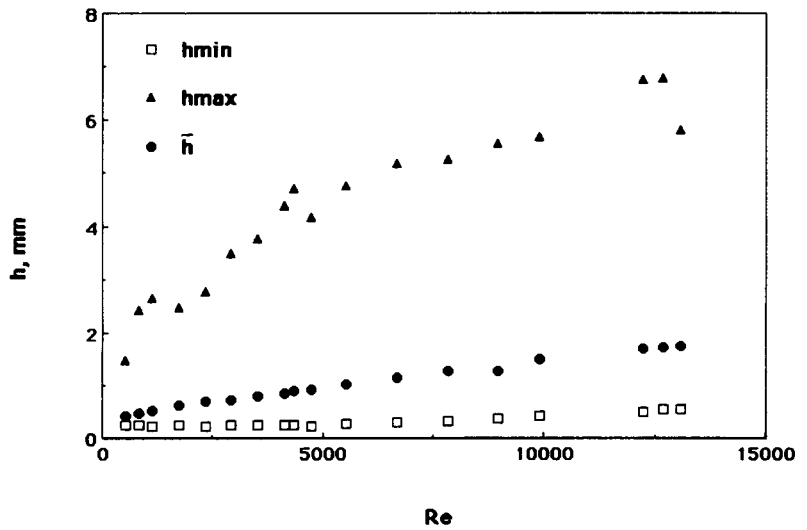

Figure 6. Maximum, minimum and mean film thickness variation with Re.

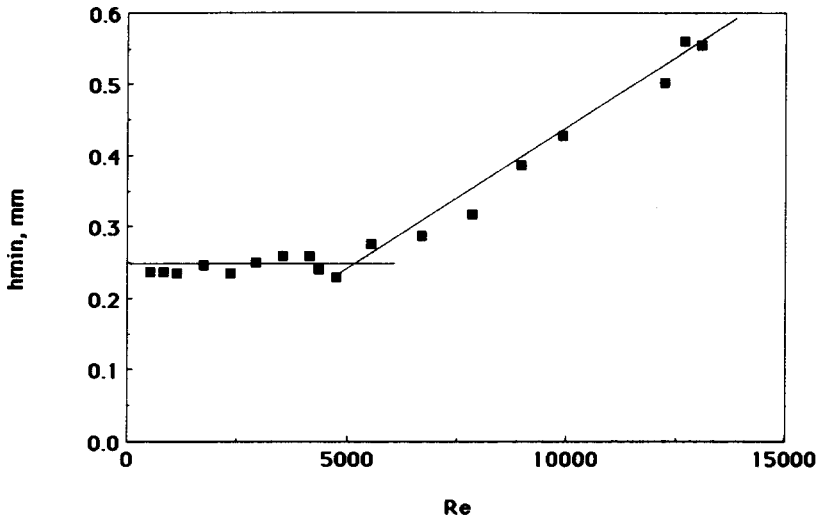

Figure 7. The minimum film thickness variation with Re.

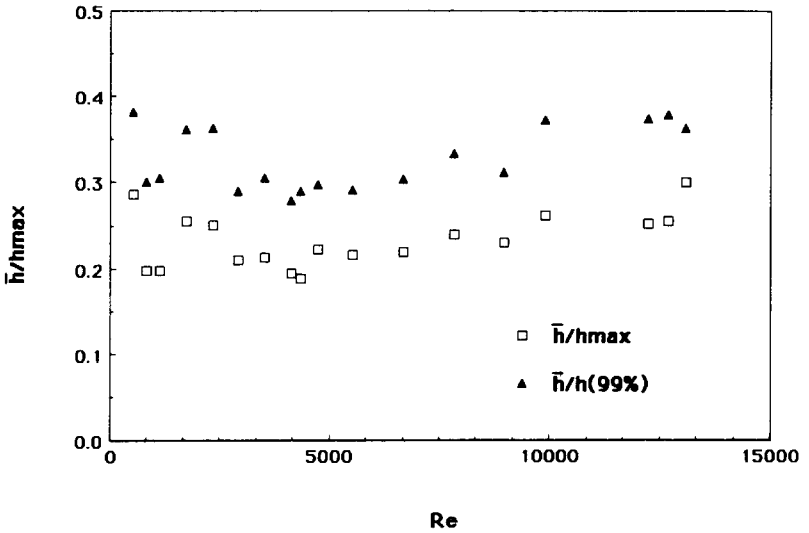

Figure 8. Ratio of mean to maximum film thickness.

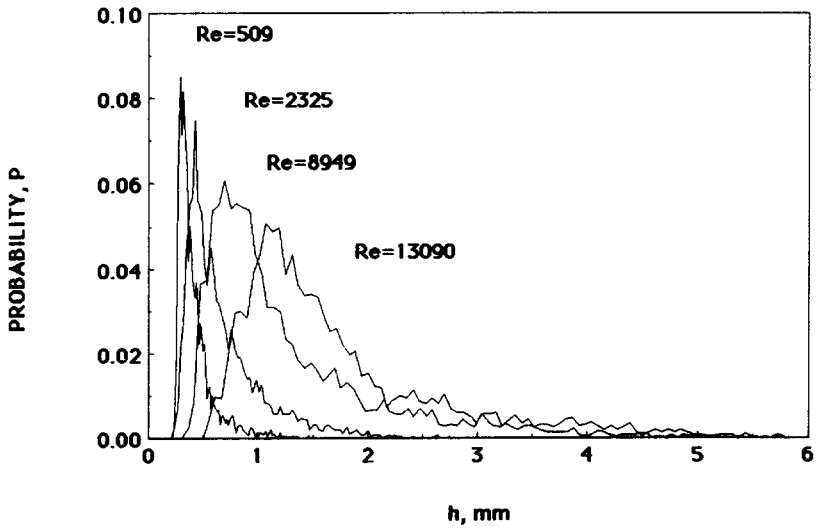

Figure 9. The effect of Re on probability density distributions.

often used measure of skewness, defined by means of the third and second central moments, is the coefficient of skewness,

$$a_3 = \frac{m_3}{\sqrt{m_2^3}}. \qquad [10]$$

The data in figure 10 show that for Re $\gtrsim$ 2000 the coefficient of skewness remains nearly constant.

Another measure of the deviation from the normal distribution is the ratio of the mean value $\bar{h}$ to the most frequent (modal) value. In the measured distribution of figure 9, this ratio is greater than unity. The influence of Re on the modal value is rather significant; namely the modal value itself tends to increase, whereas the probability corresponding to it tends to decrease with Re. It is interesting that this maximum probability is relatively low in all cases, varying between 8 and 5% in the range Re = 509 to 13,090.

The narrowest distributions with the highest peaks appear at low Re. The term kurtosis is usually employed to express the degree of "peakedness" of a distribution, taken relative to a normal distribution. The measure of kurtosis used here is the coefficient a_4, based on the normalized fourth central moment,

$$a_4 = \frac{m_4}{m_2^2} - 3. \qquad [11]$$

Figure 10 shows that for Re $\geqslant$ 2000 the coefficient of kurtosis remains nearly constant. However, the relatively high and sharp peaks observed in the measured density distributions, at low Re, result in high values of this coefficient a_4 for Re $\leqslant$ 2000.

Chu & Dukler (1974) attach special significance to the modal thickness in their classification of waves into two categories, i.e. the large and the small which cover the substrate. They assume that the probability density of the substrate is symmetrical around a mean value h_s which they set equal to the modal value of the entire distribution. This appears to be a physically realistic assumption. However, the modal values they present are very small compared to our data and to those of Takahama & Kato (1980). In figure 11 the modal values taken from Chu & Dukler's (1975) figure 4 are compared with our data, showing a large deviation. Similarly, the mean thickness values $\bar{h}$ inferred from their data are quite small, compared to widely accepted relations, as has already been pointed out in section 1.

The most frequent thickness values from this study, shown in figure 11, tend to increase almost linearly with Re over the entire Re range. The scatter in these data is due to the fact that a single

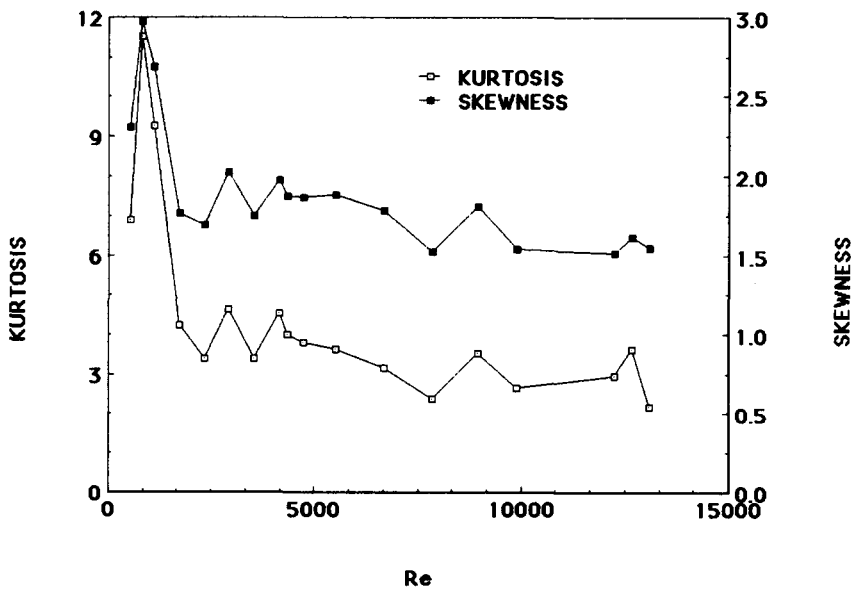

Figure 10. Skewness and kurtosis of probability density distributions of film thickness.

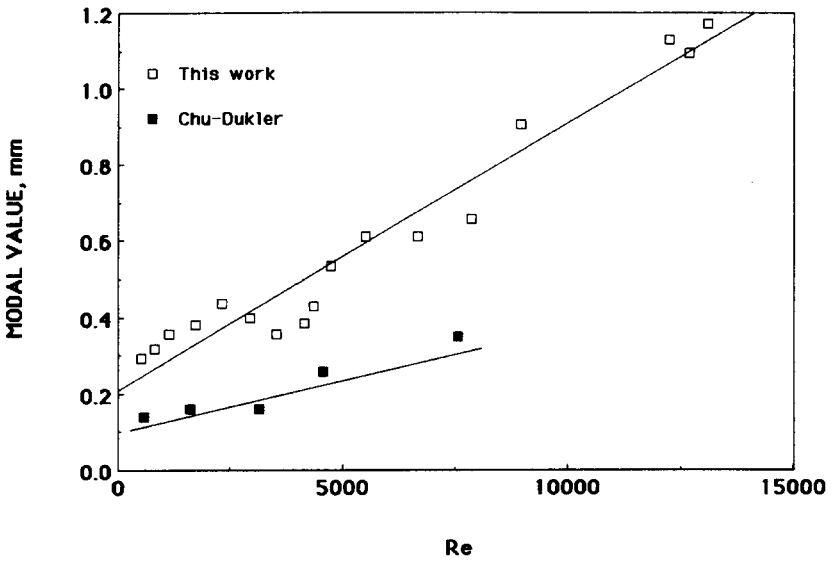

Figure 11. Influence of Re on the most frequent (modal) values of thickness obtained in this study and by Chu & Dukler (1975).

modal value was computed directly from the data. Another approach would be to do some smoothing in the probability distributions and then to select the modal value from the narrow range of most probable thickness values.

Seven measured cumulative probability distributions $\tilde{F}$, covering the entire Re range of the experiments, are presented in figure 12, along with the mean thickness value $\bar{h}$ of each distribution. It is important to note that the probability $\tilde{F}$ corresponding to the mean value $\bar{h}$ is essentially independent of Re, with a nearly constant value between $\tilde{F} = 0.65$ and 0.70. Takahama & Kato (1980) also obtain the same trend in their data, although their value is between $\tilde{F} = 0.60$ and 0.65.

The constant value of $\tilde{F}$ corresponding to $\bar{h}$ implies that waves with peak value greater than the mean have the same relative contribution to the film thickness distribution, independent of the Re. Furthermore, these large waves may have the same percentage of participation in the transportation of mass.

A careful attempt was made to determine how well theoretical distributions such as the normal, log-normal, gamma, Weibull and beta fit the measured distributions. The best fit in the range $509 \leqslant \mathrm{Re} \leqslant 9000$ was obtained with the *Weibull* distribution (e.g. Derman *et al.* 1973):

$$f(h) = \left(\frac{b}{a}\right)\left(\frac{h - h_{\min}}{a}\right)^{b-1} \cdot \exp\left[-\left(\frac{h - h_{\min}}{a}\right)\right]^{b}, \qquad \text{for } h \leqslant h_{\min}, \qquad [12]$$

where

$$a = \frac{\bar{h} - h_{\min}}{\Gamma\left(1 + \frac{1}{b}\right)}, \qquad \Gamma = \text{gamma function}$$

and

$$b \Rightarrow \frac{\Gamma\left(1 + \frac{1}{b}\right) \cdot \Gamma\left(1 + \frac{1}{b}\right)}{\Gamma\left(1 + \frac{2}{b}\right)} = \frac{(\bar{h} - h_{\min})^2}{s^2 + (\bar{h} - h_{\min})^2}.$$

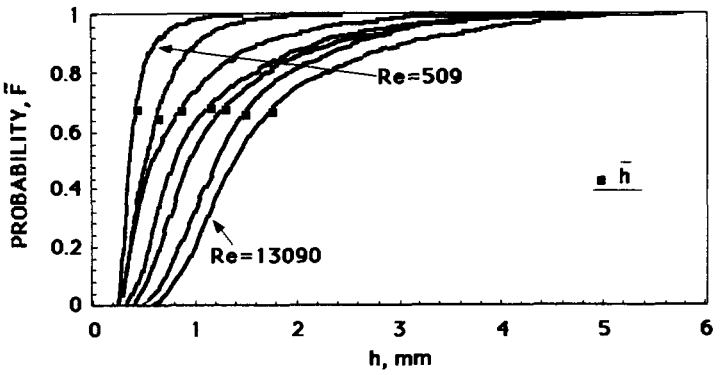

Figure 12. Measured cumulative probability density distributions at Re = 509, 1720, 4140, 6680, 8949, 9897 and 13,090.

For the range $9000 < \mathrm{Re} \leqslant 13{,}090$ the best fit was obtained with the log-normal distribution:

$$f(h) = \frac{1}{\sqrt{2\pi h^2 \delta^2}} \exp\left\{ -\left(\frac{1}{2\delta^2}\right) \cdot [\ln(h) - \xi]^2 \right\}, \qquad \text{for } h \geqslant 0, \qquad [13]$$

where

$$\delta^2 = \ln\left(\frac{s^2}{\bar{h}^2} + 1\right)$$

and

$$\xi = \ln\left(\frac{\bar{h}^2}{\sqrt{\bar{h}^2 + s^2}}\right).$$

Figure 13 shows two measured distributions at Re = 1720 and 12,245 fitted with the Weibull and log-normal distributions, respectively. Takahama & Kato fitted their data at $x = 1.7$ m with the following distributions:

$$\begin{aligned} \mathrm{Re} &\leqslant 2400, \text{ gamma} \\ 2400 < \mathrm{Re} &\leqslant 4000, \text{ log-normal} \\ 4000 < \mathrm{Re} &\leqslant 8000, \text{ gamma.} \end{aligned}$$

Telles & Dukler (1970) reported a satisfactory fit of their data in the range $1150 \leqslant \mathrm{Re} \leqslant 5750$ with the gamma distribution.

5.5. Autocovariance and spectral density functions

The autocovariance functions calculated from the data are very similar for the entire Re range of our measurements. Two typical examples, at Re = 1720 and 8949, are presented in figure 14. There is some evidence of periodicity in these graphs which may be attributed to the dominant frequency of the spectra as will be seen in the following spectral analysis. However, more time records, of size larger than that obtained in our study, are required to test the validity of this observation.

Autocovariance functions for falling films, such as those plotted in figure 14, have not been presented in the literature so far. Only Zabaras (1985) simply reports (p. 66) that, in all his cases, the autocovariance functions drop rapidly to zero.

The spectral density functions of figures 15 and 16 have been obtained as follows. A "direct Fourier transform" is employed after dividing the sample of 4000 points into seven groups of 512 points, adding zeros to the data sequence up to 4096 points to increase the resolution and applying a Hanning window function to reduce leakage. This operation was followed by segment averaging of the seven spectra and frequency smoothing for every seven points. Therefore, the error in the computed spectra (Bendot & Piersol 1971) is 14%. The resolution of the spectra is approx. 0.12 Hz. The data have been normalized using the second central moment of film thickness. Error bars have been marked on these spectra. All the calculated spectral density functions display a very

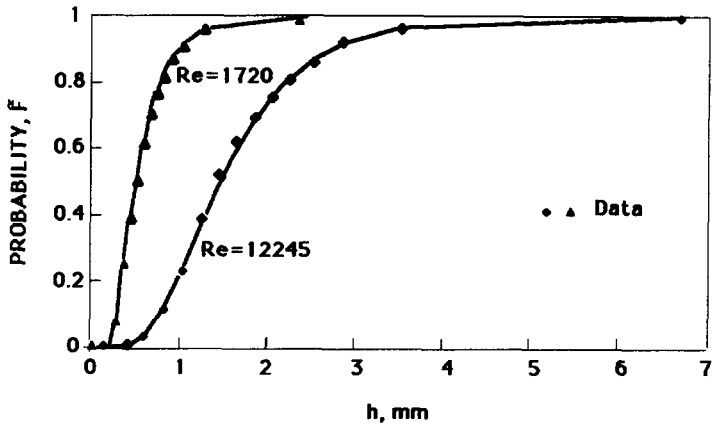

Figure 13. Successful fit of measured distributions at Re = 1720, with the Weibull, and at Re = 12,245, with the log-normal distribution.

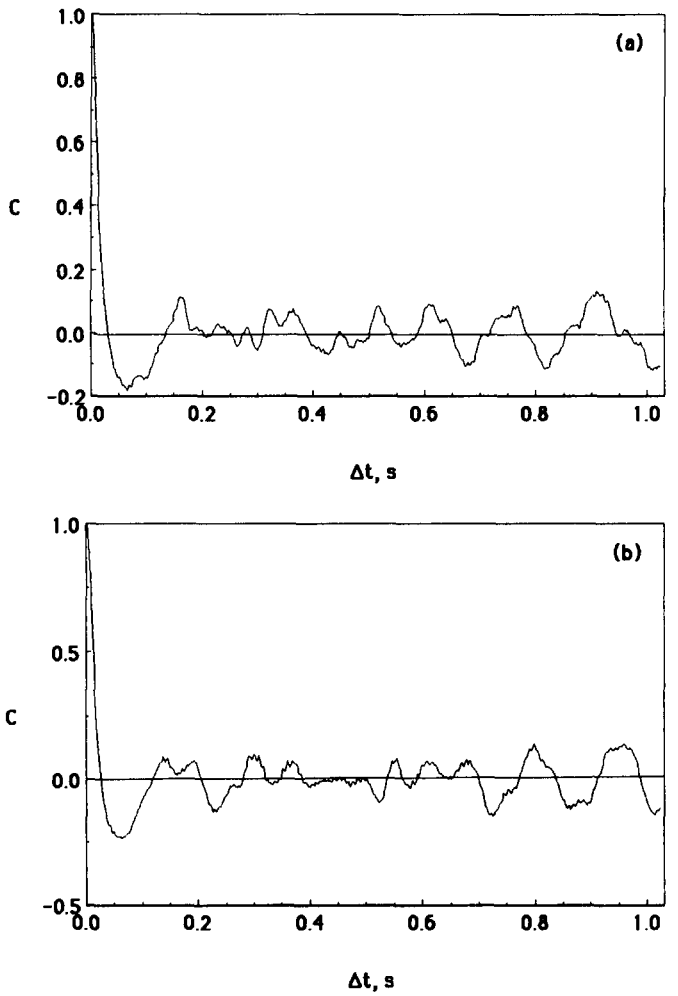

Figure 14. Autocovariance of film thickness fluctuations at (a) Re = 1720 and (b) Re = 8949.

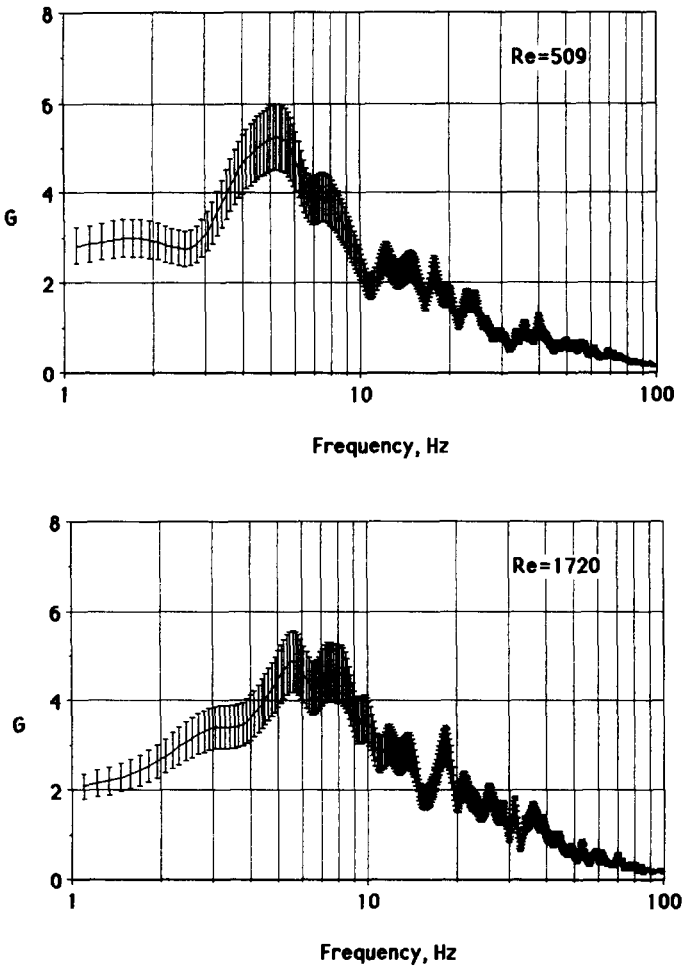

Figure 15. Spectral density functions at Re = 509 and 1720.

pronounced maximum at a frequency between 5 and 8 Hz. This modal frequency f_m is apparently characteristic of the large (roll) waves and seems to be practically independent of the Re. Indeed, by examining the traces, such as those in figure 1, one can recognize this characteristic frequency of large waves.

Chu & Dukler (1975) present spectra which exhibit modal frequencies between 2 and 5 Hz for Re = 570 to 7560. These data show a very slight increase of modal frequency with Re. Takahama & Kato (1980) have obtained a modal frequency at $f_m \approx 10$ Hz for Re = 2052. Spectra reported by Zabaras (1985) at Re = 768 and 3100 show that $f_m \approx 6$ Hz.

Another interesting feature of the spectral density functions obtained in this study (but not observed in previously published work) is a second weaker peak appearing in the frequency range 10–20 Hz. This second characteristic frequency becomes somewhat more pronounced with increasing Re and it is very likely related to smaller waves developing between the roll waves.

The shapes of the spectra shown in figures 15 and 16 are very similar at the higher frequencies, i.e. >30 Hz. In this frequency range there is an almost linear variation of the spectral density function with frequency for all Re. The spectra reported by Takahama & Kato at Re = 2052 (in their figure 9) and Zabaras at Re = 768 and 3100 (in his figures 4.17 and 4.18) display the same—nearly linear—variation at the high frequencies, but not the secondary maximum observed in our spectra.

Contrary to these results, Chu & Dukler (1975) report a much higher slope of their spectra (approx. -2.85) in the range $30 < f < 60$ Hz and for Re = 211 to 6790. They suggest that, in this so-called "equilibrium range", the slope of their spectra ($-8/3$) falls between that proposed by Phillips (1958) for wind-generated waves ($-15/3$), where gravity forces are important, and the slope

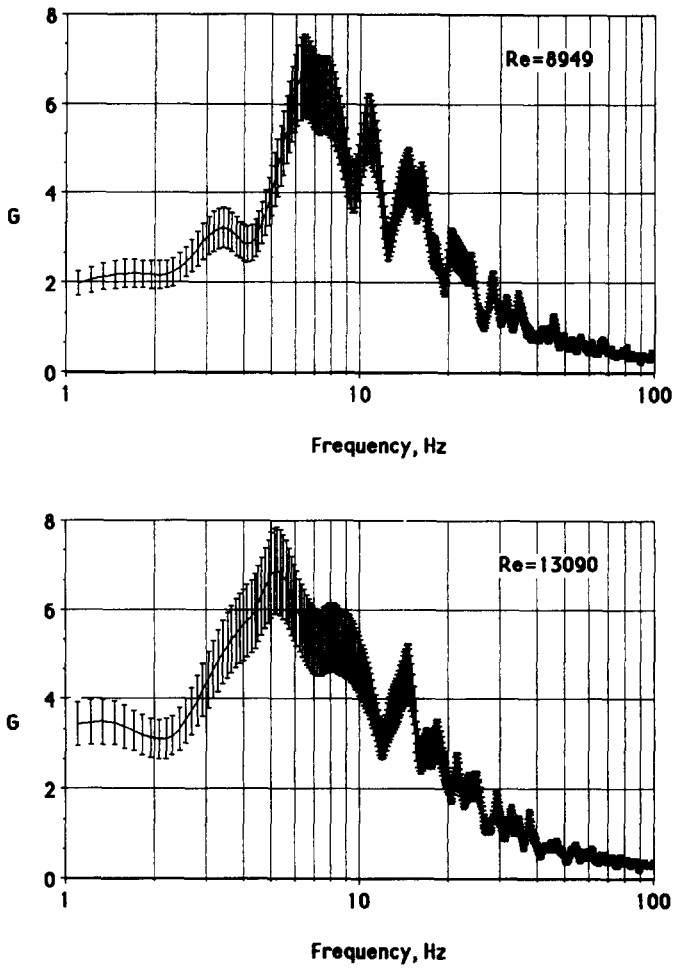

Figure 16. Spectral density functions at Re = 8949 and 13,090.

(−7/3) proposed by Hicks (1963) for capillary waves. No explanation can be offered at this time regarding the above differences in the slope of the equilibrium range.

The similarity of the spectra obtained over a wide Re range implies that the general pattern of wave energy distribution among various frequencies is essentially unaffected by the mean flow rate. Most of the wave energy is carried by waves of frequency <20 Hz, with the greatest contribution made by the large waves of frequency <10 Hz.

6. SURFACE WAVES

In the preceding statistical analysis some information about film surface waves is obtained in an indirect way, i.e. by interpreting the form of spectral density functions. Results are presented here by directly identifying the waves from the time series data $h(t)$.

Dukler and his co-workers classify a wave as *large* only if its peak height exceeds the mean film thickness $\bar{h}$ and, at the same time, the two local minima at the front and the back of the wave are *both* smaller than $\bar{h}$. These criteria seem to perform quite well at low Re. However, at moderate and especially large Re their validity may be questioned; e.g. these criteria would exclude relatively large waves, arising from the substrate, with peak height not exceeding $\bar{h}$, or waves with only one of the local minima above $\bar{h}$ (see figure 1).

A different criterion is used here to identify the waves. A wave peak h(peak) is recognized if the film height at least 0.015 s before and 0.015 s after this point is smaller than h(peak). Thus, each wave corresponds to a minimum time period of 0.03 s. The justification for using this criterion is

Table 1. Number of waves identified in a sample of 3500 data points

Re	No. of waves
509	113
812	115
1720	134
2325	122
3535	123
4355	121
5517	130
7842	127
9897	130
12,245	126
13,090	135

as follows. From the measured probability distributions of film height, a maximum probability of about 6.5% was obtained (on the average) for all Re. In the extreme case that this maximum probability corresponds to peak values, h(peak), it means that in a sample of 1000 points 65 points would represent wave peaks. The 1000 points are equivalent to 2 s for the sampling frequency of 500 Hz, used in our study. Therefore, a measure of the minimum time period separating the peaks would be $(2/65) \approx 0.03$ s. This period of 0.03 s corresponds to 15 data points in our experiments.

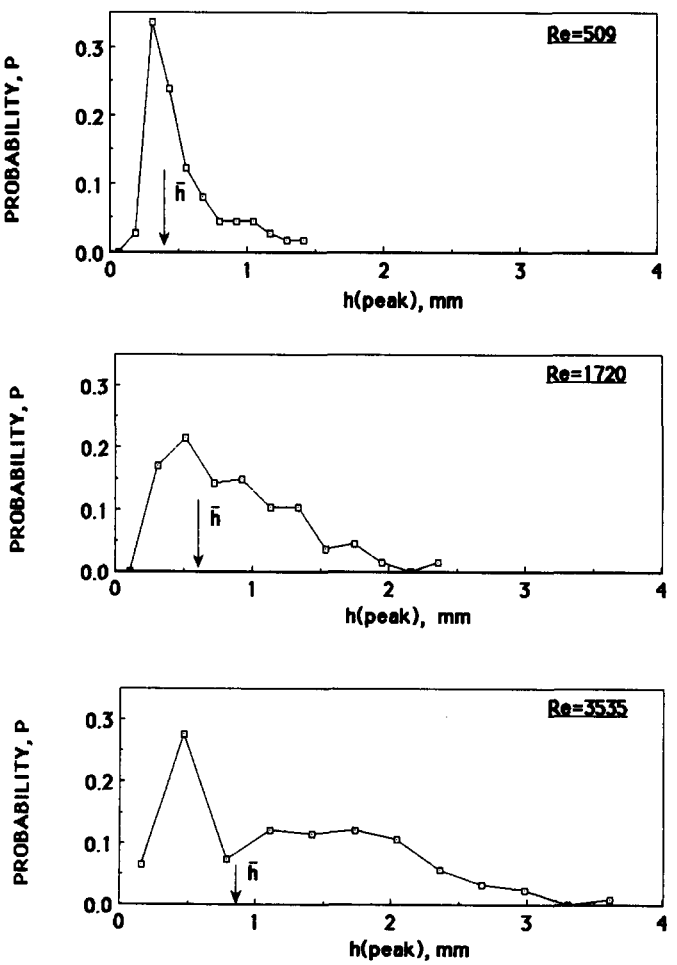

Figure 17. Probability density distributions of wave peaks at low and intermediate Re.

With the above criterion very small surface ripples are not classified as waves. By inspecting the traces one gets the impression that such ripples are evenly distributed throughout the film surface. A surprising result is obtained by counting the peaks in samples of 3500 points, as shown in table 1; i.e. for Re between 1720 and 13,090 the number of peaks appears to be almost constant varying randomly between 121 and 135. In laminar film flow (Re = 509 and 812) this number is slightly smaller (113 and 115 peaks).

Figures 17 and 18 display probability density distributions of wave peaks for six Re covering the range of our measurements. The mean thickness $\bar{h}$ is also marked in each case. For small Re, i.e. laminar flow, the distribution is relatively narrow and unimodal, with the most frequent value close to the mean $\bar{h}$. In the transition region, e.g. Re = 1720, the distribution is still unimodal but much broader. For Re > 2000, the distribution becomes wider and a second most frequent region develops. For Re > 5000, the curves display two very pronounced maxima, thus becoming bimodal.

The location of the two peaks, relative to the mean value $\bar{h}$, shows that both small and large waves (according to the Chu & Dukler criteria) have been identified with our criterion. It is worth mentioning here that Chu & Dukler (1975) obtained bimodal distributions of *large* wave amplitudes, for Re = 1025 to 6100. Even a third mode appeared in their distributions at Re $\approx$ 3000, attributed to wave coalescence. At Re = 570 the distribution was unimodal. Although not directly comparable, these distributions bear some similarities to those of figures 17 and 18. However, Chu & Dukler's suggestion that the wave amplitude distributions tend to become uniform for Re greater than those they used (Re > 6100) is not confirmed by our data, which show that the bimodal distribution persists up to Re = 13,090.

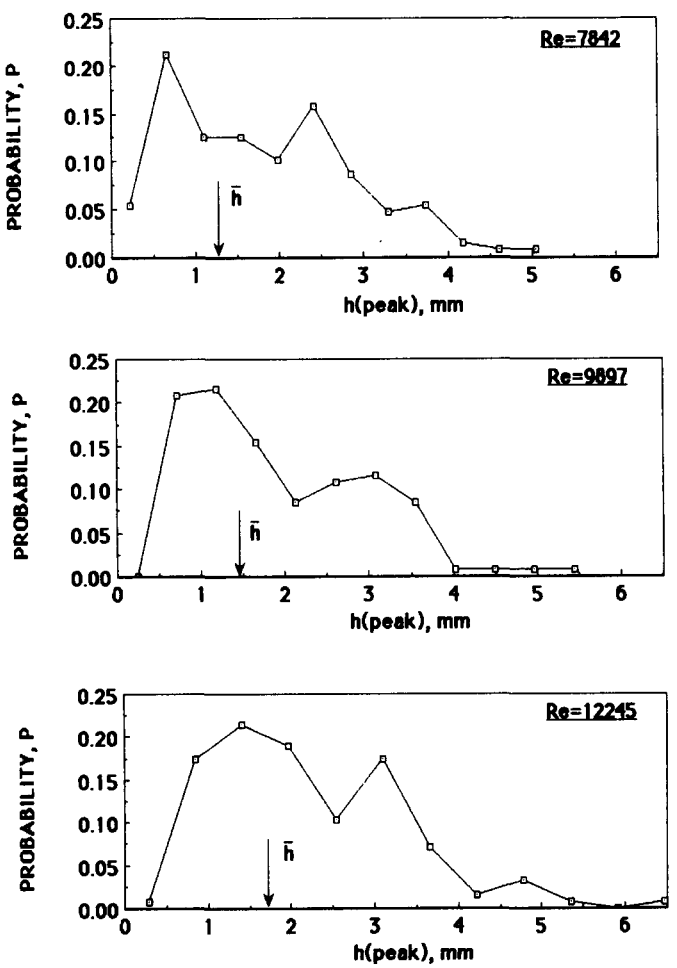

Figure 18. Probability density distributions of wave peaks at high Re.

7. SUMMARY AND DISCUSSION OF RESULTS

Visual observations suggest that at $\mathrm{Re} \gtrsim 1500$ the random character of film flow becomes pronounced, which is an indication of transition to another flow regime. The data on mean film thickness $\bar{h}$ tend to support this observation, showing a substantial deviation from the Nusselt relation for $\mathrm{Re} \gtrsim 2000$. On the contrary, no evidence of transition can be found by inspecting the $h(t)$ traces, for Re as high as 7000. The general pattern of large roll waves and of a substrate with smaller waves, described by Chu & Dukler (1974, 1975), is clearly evident in the traces up to that Re. However, for higher Re the notion of a substrate tends to break down, as the smaller waves on it are greatly amplified, attaining amplitudes comparable to the "large" waves.

The area of the wavy surface was found to be practically equal to the area computed on the basis of the mean film thickness—a result already obtained in previous investigations (e.g. Takahama & Kato 1980).

The mean thickness data, obtained over a wide Re range, are in good overall agreement with other data from the literature as well as with established relations. At low Re, our data fall above the Nusselt line which is valid for laminar film flow. However, the opposite trend is observed in some other literature data. At present this difference cannot be simply attributed to experimental errors on either side and more precise data are needed to resolve it.

The new data of some characteristic film thickness parameters such as standard deviation s, $s/\bar{h}$, $h_{\max}$ and $h_{\min}$ provide interesting information. The Re number has a rather strong influence on the standard deviation s only up to about 5000. Above this number, s increases very little showing a tendency to reach an asymptotic value. Similarly, the ratio $s/\bar{h}$ tends to increase with Re up to about 4000, to reach a maximum between 4000 and 5000, and to decrease at higher Re. The minimum thickness $h_{\min}$ is practically constant up to $\mathrm{Re} \approx 5000$ and increases at higher Re. The maximum thickness $h_{\max}$ tends to increase with Re, but this influence is drastically reduced for $\mathrm{Re} > 5000$. The ratio of $\bar{h}/h_{\max}$ is surprisingly almost constant throughout the Re range, indicating the strong effect of the large roll waves on the mean thickness.

All the above data are self-consistent and suggest the following physical picture of film flow.

For Re < 5000, the large roll waves appear to dominate and to increase in amplitude, with increasing Re, but not in frequency as will be discussed below. The nearly linear increase of r.m.s. and of $s/\bar{h}$ with Re is, indeed, indicative of increasing wave amplification and of increasing wave energy carried by large waves. The constant $h_{\min}$ suggests that the substrate has a nearly constant thickness in this Re range.

For Re > 5000, the amplification of large waves seems to stop rather abruptly while the total number of waves remains almost constant and equal to that at $\mathrm{Re} < 5000$. The substrate thickness appears to grow with Re as indicated by the increasing values of $h_{\min}$. These observations combined imply that some "redistribution" of liquid takes place, i.e. from the non-growing large waves to the smaller waves and to the substrate. It is likely that the damping action of the solid wall may cause this rather striking behavior.

The measured probability density functions are asymmetric and have a shape similar to that obtained in previous studies. The highest values of skewness and kurtosis are obtained in the pseudo-laminar flow regime, i.e. for $\mathrm{Re} < 2000$. These parameters have a nearly constant value at higher Re. The most frequent (modal) values of film thickness h_{m} appear to increase, almost linearly, with increasing Re. The very low modal values h_{m} presented by Chu & Dukler (1975) give a further indication that there is a systematic error in their measurements.

The mean thickness $\bar{h}$ corresponds to a nearly constant value of the cumulative distribution, $\tilde{F} = 0.675$, throughout the Re range. A similar value was also obtained by Takahama & Kato (1980). This result is considered useful for practical calculations as well as modeling efforts.

The best fit of the measured distributions was obtained with the Weibull distribution for $509 \leqslant \mathrm{Re} \leqslant 9000$ and the log-normal for $9000 < \mathrm{Re} \leqslant 13{,}090$. Different distributions were used in previous studies.

The calculated autocovariance functions are similar throughout the Re range. A periodicity, not reported so far in the literature, is evident in these functions and may be attributed to the dominant frequency of the large waves. However, the validity of this observation should be tested with time records longer than those obtained in our work.

The spectra display a very pronounced maximum, at frequencies between 5 and 8 Hz for all Re, which is apparently representative of the large roll waves. Similar values have been obtained in previous studies. The new result obtained in this work is a second, less pronounced, peak between 10 and 20 Hz apparently related to smaller waves in the substrate.

In order to identify the waves directly from the data a criterion is used which excludes only small ripples below a certain size. The total number of waves in a sample appears to be surprisingly constant for all Re. The probability distribution of peak heights, h(peak), is unimodal at low Re and gradually develops into a bimodal distribution.

In general, the accurate data and the results of the statistical analysis obtained in this study provide new insight and a somewhat firmer basis for future modeling efforts. Additional data are certainly needed, especially on local film velocities and shear stresses.

Acknowledgements—The authors are indebted to Professor T. J. Hanratty (University of Illinois, Urbana) for making available the negative of the printed circuit for the electronic signal analyzer. Grateful acknowledgement is also made of the partial financial support provided by the General Secretariat for Research and Technology of Greece and by the European Economic Community, DG XII under Contract EN3G-0040-GR. Thanks are also due to Professor A. E. Dukler for his constructive criticism of the original manuscript.

REFERENCES

ANDRITSOS, N. 1986 Effect of pipe diameter and liquid viscosity on horizontal stratified flow. Ph.D. Thesis, Univ. of Illinois, Urbana.

BELKIN, H. H., MCLEOD, A. A., MONRAD, C. C. & ROTHFUS, R. R. 1959 Turbulent liquid flow down vertical walls. *A.I.Ch.E. Jl* **5,** 245–248.

BENDOT, J. S. & PIERSOL, A. G. 1971 *Random Data: Analysis and Measurement Procedures.* Wiley, New York.

BLASS, E. 1979 Gas/film flow in tubes. *Int. chem. Engng* **19,** 183–195.

BRAUER, H. 1956 Strömungs und Wärmeübergang bei Rieselfilmen. *Ver Deut. Ing.*, Forschungsheft 457.

CHU, K. J. & DUKLER, A. E. 1974 Statistical characteristics of thin, wavy films: part II. Studies of the substrate and its wave structure. *A.I.Ch.E. Jl* **20,** 695–706.

CHU, K. J. & DUKLER, A. E. 1975 Statistical characteristics of thin, wavy films: part III. Structure of the large waves and their resistance to gas flow. *A.I.Ch.E. Jl* **21,** 583–593.

DERMAN, C., GLESER, L. J. & OLKIN, I. 1973 *A Guide to Probability Theory and Applications.* Holt, Rinehart & Winston, New York.

DUKLER, A. E. 1977 The role of waves in two-phase flow: some new understanding. 1976 Award Lecture. *Chem. Engng Educ.* **XI,** 108–138.

DUKLER, A. E. & BERGELIN, O. P. 1952 Characteristics of flow in falling liquid films. *Chem. Engng Prog.* **48,** 557–563.

HENSTOCK, W. H. & HANRATTY, T. J. 1976 The interfacial drag and the height of the wall layer in annular flows. *A.I.Ch.E. Jl* **22,** 990–1000.

HICKS, B. L. 1963 Estimation of the spectrum function for small wind waves. In *Ocean Wave Spectra.* Prentice-Hall, Englewood Cliffs, N.J.

JACKSON, M. L. 1955 Liquid films in viscous flow. *A.I.Ch.E. Jl* **1,** 231–240.

KAPITSA, P. L. 1964 Wave flow of thin layers of a viscous fluid. In *Collected Papers of P. L. Kapitsa.* Macmillan, New York.

KARAPANTSIOS, T. D. 1987 A study of flow characteristics of a thin liquid layer in a vertical pipe. Diploma thesis in Chemical Engineering, Univ. of Thessaloniki. In Greek.

KOZIOL, K., ULATOWSKI, J. & FRANKE, K. 1981 Velocity field in falling films. *Int. chem. Engng* **21,** 580–584.

MARON, D. M., BRAUNER, N. & DUKLER, A. 1985 Interfacial structure of thin falling films: piecewise modelling of the waves. *PhysicoChem. Hydrodynam.* **6,** 87–113.

MIYA, M., WOODMANSEE, D. E. & HANRATTY, T. J. 1971 A model for roll waves in gas–liquid flow. *Chem. Engng Sci.* **26,** 1915–1931.

MUDAWWAR, I. A. & EL-MASRI, M. A. 1986 Momentum and heat transfer across freely-falling turbulent liquid films. *Int. J. Multiphase Flow* **12,** 771–790.

NUSSELT, N. 1916 Die Oberflächenkondensation der Wasserdampfes. *Zeit. Ver. D. Ing.* **60,** 541–569.

PARAS, S. V. 1988 A study of horizontal annular flow. Ph.D. Thesis, Univ. of Thessaloniki. In preparation.

PHILLIPS, O. M. 1958 The equilibrium range of wind generated waves. *J. Fluid Mech.* **4,** 426–434.

PIERSON, F. W. & WHITAKER, S. 1977 Some theoretical and experimental observations of the wave structure of falling liquid films. *Ind. Engng Chem. Fundam.* **16,** 401–408.

PORTALSKI, S. 1963 Studies of falling liquid film flow. Film thickness on a smooth vertical plate. *Chem. Engng Sci.* **18,** 787–804.

PORTALSKI, S. & CLEGG, A. J. 1972 An experimental study of wave inception on falling liquid films. *Chem. Engng Sci.* **27,** 1257–1265.

SON, J. C. & HANRATTY, T. J. 1969 Velocity gradients at the wall for flow around a cylinder at Re from 5×10^3 to 10^5. *J. Fluid Mech.* **35,** 353–368.

SWANSON, R. W. 1966 Characteristics of the gas-liquid interface in two phase annular flow. Ph.D. Thesis, Univ. of Delaware.

TAKAHAMA, H. & KATO, S. 1980 Longitudinal flow characteristics of vertically falling liquid films without concurrent gas flow. *Int. J. Multiphase Flow* **6,** 203–215.

TELLES, A. S. & DUKLER, A. E. 1970 Statistical characteristics of thin, vertical, wavy, liquid films. *Ind. Engng Chem. Fundam.* **9,** 412–321.

ZABARAS, G. J. 1985 Studies of vertical annular gas–liquid flows. Ph.D. thesis in Chemical Engineering, Univ. of Houston, Tex.